Journal of Inflammation Research

Dovepress
Taylor & Francis Group

Open Access Full Text Article

ORIGINAL RESEARCH

Cigarette Smoking Induces Skeletal Muscle Atrophy in Mice by Activated Macrophage-Mediated Pyroptosis

Yufen Tan[1,*], Yuanyuan Ye[1,*], Cuibi Huang[1], Jie Li[1], Lihua Huang[1], Xinyan Wei[1], Tong Liang[1], Enyuan Qin[1], Guolin Xiong[2], Yanfei Bin[1]

[1]Department of Respiratory and Critical Care Medicine, the second Affiliated Hospital of Guangxi Medical University, Nanning, People's Republic of China; [2]Guangxi University of Chinese Medicine, Nanning, People's Republic of China

*These authors contributed equally to this work

Correspondence: Yanfei Bin, The second Affiliated Hospital of Guangxi Medical University, Nanning, People's Republic of China, Email binyanfei@163.com; Guolin Xiong, Guangxi University of Chinese Medicine, Nanning, People's Republic of China, Email 269380705@qq.com

Objective: Skeletal muscle atrophy is a major comorbidity associated with chronic obstructive pulmonary disease caused by exposure to cigarette smoke (CS). CS-activated macrophages and pyroptosis play an important role in skeletal muscle atrophy, but its specific molecular mechanism remains unclear. This study investigated the role and mechanisms of pyroptosis and activated macrophages in CS-induced skeletal muscle atrophy.

Methods: In the in vivo model, mice were exposed to either CS or air for 24 weeks, and in the in vitro model, C2C12 murine skeletal muscle cells were co-cultured with macrophages in Transwell chambers. Western blotting, real-time PCR, ELISA, and other methods were used to detect pyroptosis-related markers to investigate the mechanism of CSE-activated macrophages on skeletal muscle atrophy and pyroptosis.

Results: In vivo, CS-induced atrophy of the mouse gastrocnemius muscle was accompanied by increased expression of pyroptosis-related markers, including NLRP3 inflammasome, cleaved Caspase-1, the GSDMD N-terminal domain, and interleukin (IL)-18. In vitro, CS extract (CSE)-activated macrophages mediates pyroptosis of skeletal muscle cells and induces myotube atrophy. Further studies demonstrated that macrophage-derived TNF-α is the initiating factor of skeletal muscle pyroptosis, and this process appears to be mediated through TNF-α activating the TNFR1/NLRP3/caspase-1/GSDMD signaling pathway.

Conclusion: TNF-α released by CSE-activated macrophages can promote skeletal muscle pyroptosis by activating the TNFR1/NLRP3/Caspase-1/GSDMD signaling pathway, which likely contributes to skeletal muscle atrophy. These findings provide more insight into the mechanisms underlying skeletal muscle atrophy in COPD.

Keywords: cigarette smoke, chronic obstructive pulmonary disease, skeletal muscle atrophy, macrophages, pyroptosis

Introduction

Chronic obstructive pulmonary disease (COPD) is one of the three leading causes of death globally, with smoking being the most important risk factor.[1] Skeletal muscle atrophy is a major comorbidity of COPD patients, and the overall prevalence varies from 15.5% to 34%.[2] Skeletal muscle atrophy can lead to reduced muscle strength and endurance, thereby decreasing quality of life and survival.[3,4] This complication is an independent predictor of mortality in patients with COPD.[5,6] However, effective pharmacologic treatments for skeletal muscle atrophy beyond exercise training are lacking. Thereby, elucidating the molecular mechanisms underlying skeletal muscle atrophy is essential for developing effective intervention strategies.

Current research suggests that an enhanced inflammatory response to oxidative stress stimuli, such as cigarette smoke (CS), leads to heightened myofibrillar protein degradation and reduced protein synthesis, which is considered the primary

Received: 9 October 2024
Accepted: 7 February 2025
Published: 19 February 2025

mechanism of skeletal muscle wasting in COPD patients.[7,8] Muscle fiber differentiation is a critical phase in the development of skeletal muscle formation. Myogenic regulatory factors (MRFs), including myoblast determination protein (MyoD), myogenin (MyoG), myf-5 and MRF4, are the main muscle-specific transcription factors in the MyoD family, and play crucial roles in the regulation of myogenesis.[9] Myogenin, which is ubiquitously expressed in all skeletal muscles, is a key driver of the terminal differentiation of myocytes. These MRFs are also instrumental in the repair of muscle damage.[10,11]

CS-induced oxidative stress attracts macrophages to accumulate in the lungs and release large quantities of inflammatory cytokines like TNF-α, as well as oxidizing substances and enzymes, leading to lung tissue damage and persistent airway inflammation.[12] These inflammatory mediators released by CS-activated macrophages are not limited to the lungs, and the "spillover"of pulmonary inflammation into the systemic circulation may cause systemic damage, including skeletal muscle, resulting in reduced differentiation of skeletal muscle.[12] In addition, sustained stimulation of CS results in increased macrophage infiltration in skeletal muscle, and locally resident macrophages are pivotal in the processes of muscle damage and repair.[13] Many studies confirmed that TNF-α promotes skeletal muscle atrophy through complex cell death signaling pathways.[14,15] Our previous study found that local inhibition of TNF-α did not reverse skeletal muscle atrophy, suggesting that systemic sources of TNF-α also play an important role.[16] Macrophages are a major cellular source of TNF-α under inflammatory states. However, whether macrophage-derived TNF-α promotes skeletal muscle atrophy and its mechanism remain unclear.

Pyroptosis represents a form of regulated necrotic cell demise, initiated by inflammatory stimuli, and is distinguished by cellular distension, cell membrane rupture, and the emission of pro-inflammatory factors. According to certain research, pyroptosis is a crucial factor in the progression of skeletal muscle atrophy under non-infectious inflammatory conditions such as dermatomyositis/polymyositis, diabetic myopathy, and glucocorticoid-associated myasthenia gravis.[17–19] The NLRP3 inflammasome is an upstream regulator of pyroptosis.[20] TNF-α is essential for the activation of the NLRP3 inflammasome, which subsequently triggers the activation of caspase-1.[21] The activated caspase-1 facilitates the maturation of the proinflammatory cytokines IL-1β and IL-18. Gasdermin D (GSDMD) is also cleaved by activated caspase-1, releasing its N-terminal domain which oligomerizes and forms pores in the cell membrane to release inflammatory molecules, such as IL-1β, inducing pyroptotic cell death.[22] Nevertheless, the role and specific mechanisms of macrophage-derived TNF-α-mediated pyroptosis in CS-induced skeletal muscle atrophy have yet to be clarified.

The present study hypothesized that skeletal muscle atrophy caused by CS is linked to TNF-α released from CS extract (CSE)-activated macrophages and pyroptosis. In vivo, we established a mouse model of COPD to explore the role of pyroptosis in skeletal muscle atrophy. In vitro, we utilized a co-culture system of C2C12 murine skeletal muscle cells and RAW264.7 macrophages to further explore the effects and detailed molecular mechanisms of inflammatory mediators released from CSE-activated macrophages on skeletal muscle cell pyroptosis.

Materials and Methods

Reagents and Antibodies

Dulbecco's modified Eagle's medium (DMEM, C11995500BT) and fetal bovine serum (FBS, 10099141C) were purchased from Gibco (Grand Island, NY, USA). Horse serum (HS) was acquired from Vivacell (C2510-0500, Shanghai, China). Recombinant TNF-α (RP01071) was obtained from ABclonal (Wuhan, China). Infliximab (HY-P9970), MCC950 (HY-12815A), and R-7050 (HY-110203) were obtained from MedChemExpress (NJ, USA). RNA-easy Isolation Reagent (R701-02) was purchased from Vazyme (Nanjing, China). PrimeScript RT reagent (#22107) was purchased from TOLOBIO (Shanghai, China), and SYBR Premix Ex Taq kits (A304) were purchased from GenStar (Beijing, China). TNF-α and IL-1β (mouse) ELISA kits were obtained from DEVELOP (Wuhan, China). Primary antibodies against NLRP3 (ab263899), GSDMD (ab219800), and caspase-1 (ab179515) were purchased from Abcam (Waltham, MA, USA). Primary antibodies against TNF-α (60,291-1-lg), TNF receptor 1 (TNFR1, 60,192-1-lg), MyoD (18943-1-AP), and GAPDH (6004-1-lg) were procured from Proteintech (Wuhan, China). Cleaved caspase-1 (A0964), IL-1β (A11369), IL-18 (A1115), and β-actin (AC026) antibodies were purchased from ABclonal, MyoG (CY8830) was

purchased from Abways, and fluorescent secondary antibodies (#5151P) were obtained from Cell Signaling Technology (Danvers, MA, USA).

Animals

A total of 24 male mice (C57BL/6, 5–6 weeks, 18 ± 2 g) were acquired from the Guangxi Medical University Animal Research Centre (GXMU, Nanning, China), including 12 mice as the Control group and 12 mice as the CS group. All animals were housed on a 12-h light/dark cycle. The animals were exposed to either air or CS for 24 weeks according to previously described protocols.[23] At the end of the experiment, the right gastrocnemius muscle (GM) of mice was dissected for histological evaluation, and the left GM was isolated for further analysis. All animal experiments were approved by the Guangxi Medical University Laboratory Animal Committee and conducted per the requirements of the Animal Care and Use Committee (Approval NO. 202401008).

Histology

Fresh tissues were fixed with 4% paraformaldehyde overnight, dehydrated, paraffin-embedded, and serially sliced to 5 μm for Haematoxylin-eosin (HE), Masson trichrome, and immunofluorescence staining. Cross-sectional images of the GM were captured using a microscope (Olympus, Tokyo, Japan). The cross-sectional area (CSA) of the muscle fibers was calculated utilizing ImageJ software (National Institutes of Health, USA).

Cell Culture

RAW 264.7 cells (leukemia-transformed mouse macrophages, SCSP-5036) and C2C12 cells (murine myoblast cell line, SCSP-505) were obtained from the Shanghai Cell Bank, Chinese Academy of Sciences. They were cultured in DMEM supplied with 10% FBS and 1% penicillin-streptomycin. When C2C12 cells reached approximately 80% confluence, differentiation was induced via incubation in DMEM containing 2% HS for 5 days. RAW264.7 cells were seeded in the upper layer of Transwell chambers (0.4 μm, Corning, NY, USA) and co-cultured with C2C12 myotubes for 24 h. Before co-culture with RAW264.7 cells, C2C12 myotubes were preincubated with 5 μM R-7050 for 2 h (to inhibit TNFR1 activity) or 5 μM MCC950 for 1 h (to inhibit NLRP3 activity).

CSE Preparation

As previously outlined, three unfiltered full-strength burning cigarettes were sequentially connected to a pumping device with a 50-mL syringe and "smoked" slowly and repeatedly. The obtained smoke was dissolved in 3 mL of PBS to create a suspension, followed by filtration through a 0.22-μm sterile filter. The optical density of the CSE was determined, and the extract was used within 1 h.[24]

Cell Viability

RAW264.7 cells (1 × 104 /well) were stimulated with various levels of CSE (0, 0.05%, 0.1%, 0.15%, 0.2%, 0.4%) for 12 or 24 h. After incubation, 10% CCK8 solution (Dojindo, Japan) was added, and the absorbance of each well was assessed at 450 nm utilizing a microplate reader (BioTek Gen5, BioTek, Shoreline, WA, USA). Cell viability was calculated relative to the control sample.

Giemsa Staining

C2C12 cells were washed with PBS and fixed with 70% ethanol for 10 min. Subsequently, cells were mixed with 10% Giemsa staining solution (Beyotime, Shanghai, China) together for 30 min. Ultimately, the images were acquired randomly using a microscope (Olympus, Tokyo, Japan).

ELISA and Lactate Dehydrogenase (LDH) Release

Supernatants from RAW264.7 and C2C12 cell cultures were collected following various treatments. Following the manufacturer's protocol, the concentrations of TNF-α and IL-1β in the cell supernatants were determined utilizing

ELISA kits. Cell membrane damage and cell death were evaluated by measuring LDH release from C2C12 cells using an LDH assay kit (Beyotime, Shanghai, China). The OD value was measured using a microplate reader.

Western Blot

Proteins were extracted from cells and tissues and separated by SDS-PAGE. Following separation, the proteins were transferred to PVDF membranes and blocked with 5% skim milk for 1 h. Subsequently, the membranes were incubated with primary antibodies against TNF-α (1:1500), TNFR1 (1:2500), NLRP3 (1:1000), GSDMD (1:8000), the GSDMD N-terminal domain (GSDMD-N, 1:800), caspase-1 (1:10,000), cleaved caspase-1 (1:10,000), IL-1β (1:1000), IL-18 (1:1000), MyHC(1:2000), MyoD(1:4000), MyoG(1:1500), β-actin (1:300,000), and GAPDH (1:300,000) overnight at 4°C. Next, the membranes were incubated with fluorescently secondary antibodies (1:30,000) at room temperature for 1 h. The proteins were visualized using Odyssey Infrared Fluorescence Scanning Imaging System (US National Institutes of Health, Bethesda, MD, USA).

Real-Time PCR (RT-PCR)

Total RNA was isolated from cells subjected to different treatments using the RNA-easy Isolation Reagent and then reverse transcribed to cDNA. The SYBR Green PCR kit was utilized to semi-quantify the gene levels relative to housekeeping gene GAPDH. The primer sequences used are provided in Table 1.

Propidium Iodide (PI) Staining

Following the previous treatments, C2C12 cells were cultured in staining buffer containing PI (Beyotime, Shanghai, China) and then analyzed for fluorescence using a fluorescence microscope (EVOS® FL Auto Imaging System).

Table 1 Sequences of RT-PCR Primers

Gene product		Sequences
TNF-α	Forward (5′ to 3′)	CACGCTCTTCTGTCTACTGAACTTC
	Reverse (5′ to 3′)	CTTGGTGGTTTGTGAGTGTGAGG
TNFR1	Forward (5′ to 3′)	AGAGAAAGTGAGTGCGTCCCT
	Reverse (5′ to 3′)	ACCTGAGTCCTGGGGGTTTG
NLRP3	Forward (5′ to 3′)	GCTGTGTGTGGGACTGAAGCA
	Reverse (5′ to 3′)	CTGACAACACGCGGATGTGA
Caspase-1	Forward (5′ to 3′)	GGACCCTCAAGTTTTGCCCT
	Reverse (5′ to 3′)	GCAAGACGTGTACGAGTGGT
GSDMD	Forward (5′ to 3′)	GATCAAGGAGGTAAGCGGCA
	Reverse (5′ to 3′)	CACTCCGGTTCTGGTTCTGG
IL-1β	Forward (5′ to 3′)	CCAGGATGAGGACATGAGCAC
	Reverse (5′ to 3′)	TGTTGTTCATCTCGGAGCCTGTA
IL-18	Forward (5′ to 3′)	ACAATGGCTGCCATGTCAGAA
	Reverse (5′ to 3′)	TTGTACAGTGAAGTCGGCCAAAG
GAPDH	Forward (5′ to 3′)	ATCACTGCCACCCAGAAG
	Reverse (5′ to 3′)	TCCACGACGGACACATTG

Knockdown of TNF-α in Macrophages

TNF-α knockdown lentivirus (TNF-α-shRNA sequence: 5′-GCCGATTTGCTATCTCATACC-3′) and the empty lentiviral vector (negative control-shRNA) were produced by GENECHEM (Shanghai, China). The lentiviruses were transfected to RAW264.7 cells for 16 h. Subsequently, the cells were incubated for 72 h and then selected with 3 μg/mL puromycin to screen for stable knockdown of TNF-α in cell lines.

Immunofluorescence

GAS muscle sections or C2C12 myotubes were fixed with 4% paraformaldehyde for 15 min and permeabilized with 0.25% Triton X-100 for 20 min. After blocking with 3% BSA, the cells were incubated overnight at 4°C with primary antibodys such as against myosin heavy chain 1 (MHC1, 1:250, Santa Cruz, Dallas, TX, USA) and dystrophin (1:100, Servicebio, Wuhan, China), and then incubated with Cy3-labeled secondary antibody (1:500, Beyotime, Shanghai, China). The nuclei were stained by DAPI (Beyotime). Ultimately, the images were documented using a fluorescence microscope.

Statistical Analysis

The data were expressed as the mean ± standard deviation (SD). Statistical significance between two groups was assessed using Student's *t*-test, while one-way ANOVA was applied for multi-group comparisons. $P < 0.05$ was considered statistically significant.

Results

Chronic CS exposure induces skeletal muscle atrophy accompanied by enhanced expression of pyroptosis-related proteins in mice

Body weight and the morphology and weight of the GM were assessed in mice exposed to CS or air. Exposure to CS resulted in weight loss compared to the control group (Figure 1A). In addition, CS exposure significantly reduced GM weight in mice (181.25 ± 4.59 mg vs 139.75 ± 5.65 mg, Figure 1B and C). HE staining, Masson trichrome, and dystrophin staining revealed that the GM fibers of CS-exposed mice exhibited signs of atrophy and a disordered fiber arrangement. In addition to this, the results showed that the CSA of gastrocnemius muscle was significantly reduced in CS-exposed mice compared to the control group. The CSA of GM fibers in the control group was mainly 800~1200 μm^2, and the CSA of GM fiber in the CS group was concentrated in the range of 400~800 μm^2 (Figure 1D). Dystrophin is an anti-atrophy protein primarily distributed beneath the sarcolemma of skeletal and cardiac muscles, where it binds to the extracellular matrix in a specific manner to maintain the integrity of the muscle cell membrane. Immunofluorescence staining shows that dystrophin was positively expressed on the muscle cell membrane, and continuous and complete annular fluorescence was seen on the muscle membrane of the control group, indicating that the muscle membrane of the gastrocnemius muscle of the control group was intact. However, the intensity of dystrophin was lower in the CS group, and the fluorescence on the muscle membrane was discontinuous and disconnected. These indirectly suggests that CS causes damage to the integrity of mouse skeletal muscle (Figure 1E). Next, to explore the impact of prolonged CS exposure on muscle specific gene expression, we analyzed the protein expression of MyHC, MyoD, and myogenin in mouse GM tissue from Control and CS. The results showed that the protein expression of MyHC, MyoD, and MyoG was reduced in GM in the CS group compared to the control group (Figure 1F and G), suggesting that CS exposure decreases muscle fiber differentiation capacity. Chronic CS exposure induces skeletal muscle atrophy. To explore the impact of prolonged CS exposure on muscle pyroptosis, we focused on the expression of pyroptosis-related molecules in GM. Compared to the control group, the expression of NLRP3, GSDMD-N, and cleaved caspase-1 in the GM was increased in the CS group (Figure 1H and I). In addition, CS exposure significantly enhanced the expression of IL-18 and TNF-α in GM (Figure 1J and K). These results suggest that CS-induced enhanced expression of pyroptosis-related proteins, which may be related to skeletal muscle atrophy.

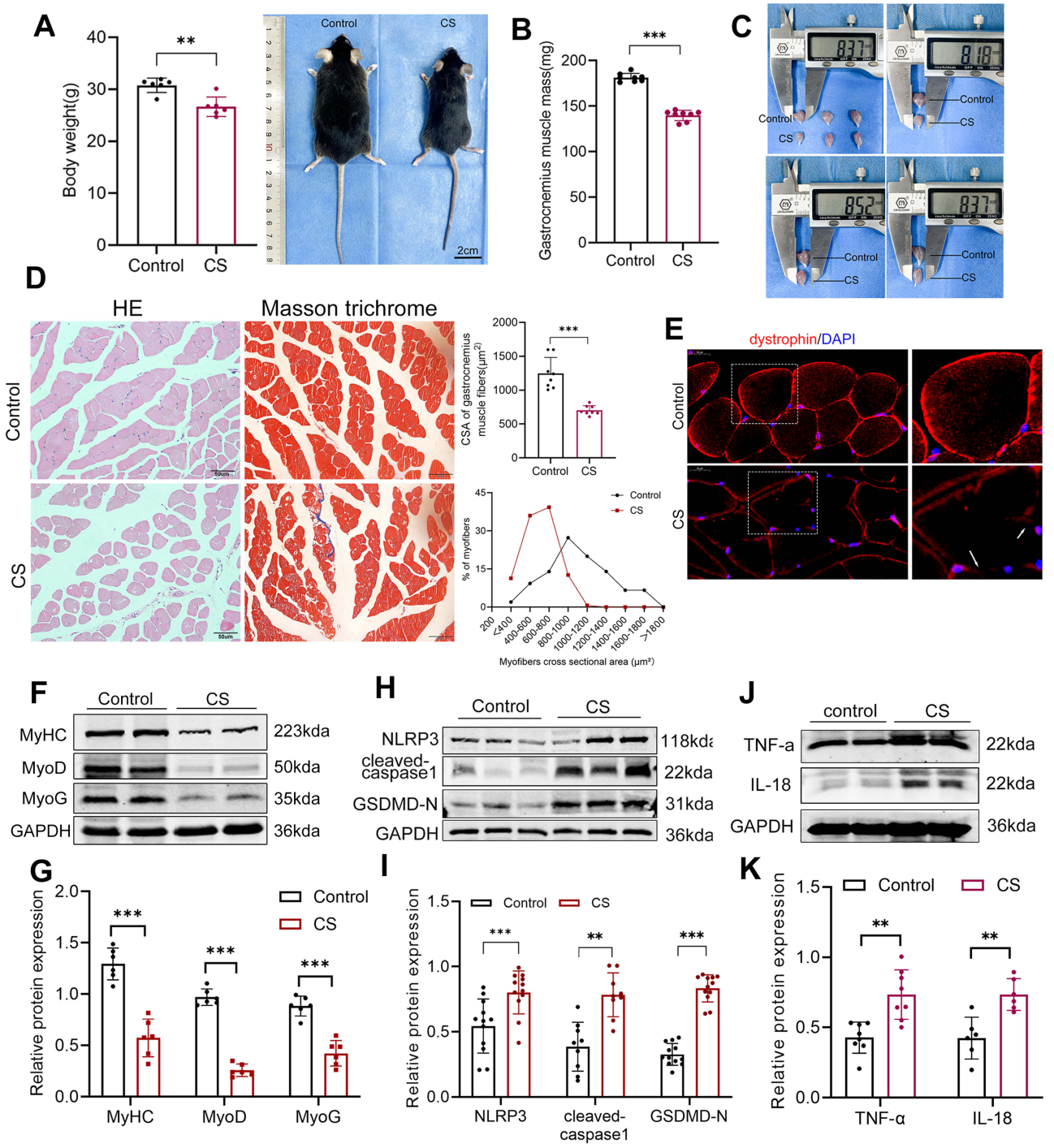

Figure 1 Chronic CS exposure induces skeletal muscle atrophy and enhances the expression of pyroptosis-related proteins in mice. (**A**) Body weight of mice exposed to room air or CS for 24 weeks (n=6). (**B**) GM weight (n=8). (**C**) Representative GM dissection samples in the control and CS groups (n=6). (**D**) HE staining and Masson's trichrome staining images of the GM fibers along with muscle fiber CSA in mice exposed to room air or CS (n=8). Scale bars: 50 μm. (**E**) Dystrophin immunofluorescence staining was used to analyze the CSA of GM fibers and visualize the cell membrane (n=8). White arrows indicate the rupture of gastrocnemius muscle membrane. Scale bars: 20 μm. (**F–K**) The protein expression of MyhC, MyoD, MyoG, NLRP3, cleaved caspase-1, GSDMD-N, TNF-α, and IL-18 in the GM tissue of mice exposed to room air or CS (n=6~12). All experiments were repeated three times with consistent results. $^{**}P < 0.01$, $^{***}P < 0.001$.

CSE-Activated Macrophages Promote C2C12 Myotube Pyroptosis

Based on the observed increase in pyroptosis in the GM of mice following chronic CS exposure, C2C12 cells were used to further dissect the mechanisms by which CS exposure causes skeletal muscle atrophy in vitro. Giemsa staining

revealed that C2C12 myoblasts were spindle-shaped mononuclear cells, and C2C12 myotubes were multinucleated cells with elongated morphology (Figure 2A). Using specific monoclonal antibodies targeting MHC1, a specific myotube marker, the morphological differentiation of C2C12 myotubes used in subsequent experiments was confirmed through immunofluorescence staining (Figure 2B).

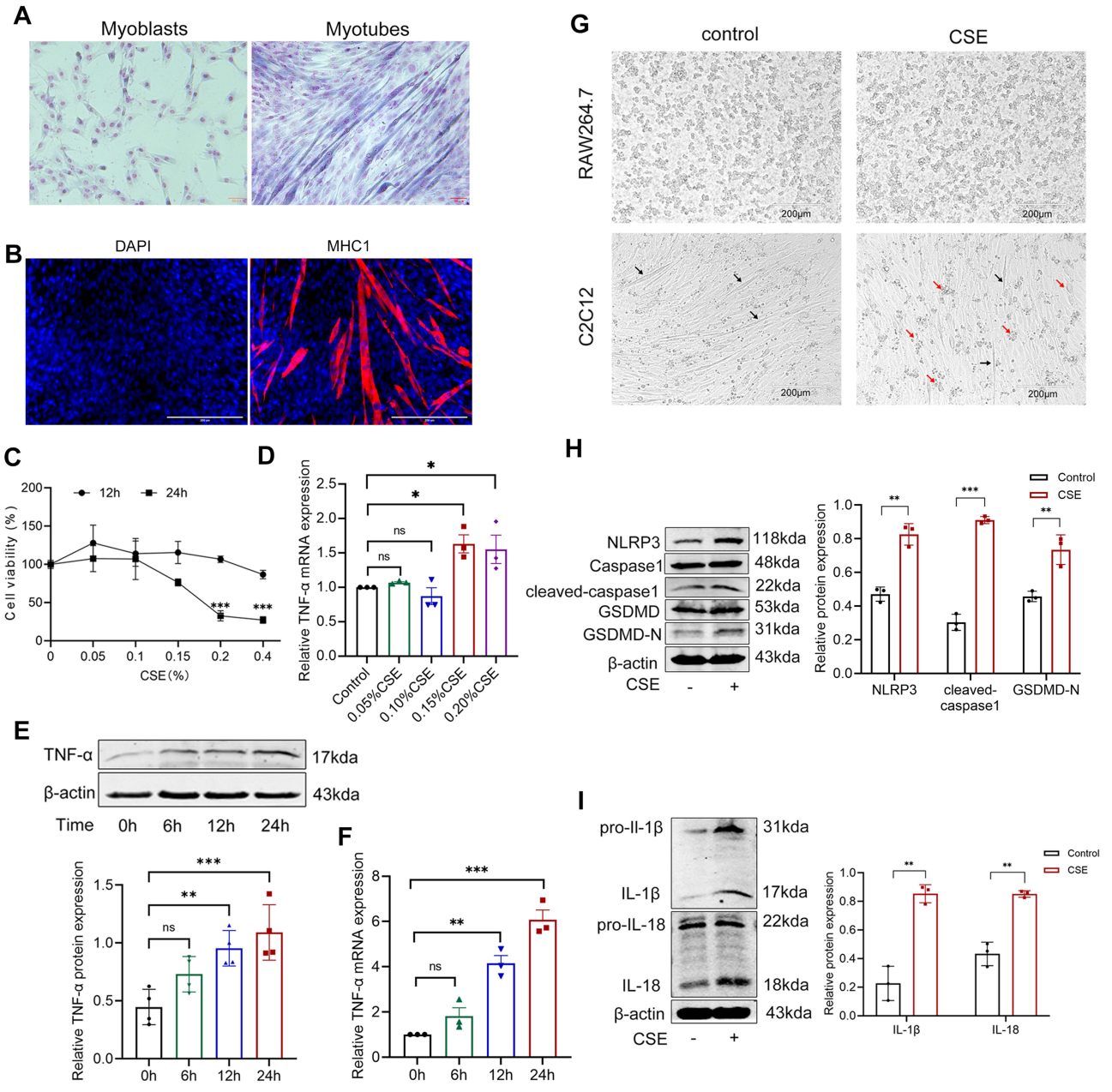

Figure 2 CSE-activated macrophages promote C2C12 myotubes pyroptosis. (A) The Giemsa staining morphology of C2C12 myoblasts and myotubes. Scale bar: 50 μm. (**B**) Immunofluorescence staining of C2C12 myotubes for MHC1 (red). Nuclei were stained with DAPI (blue). Scale bar: 200 μm. (**C**) viability of RAW264.7 cells treated with CSE (0.05%, 0.1%, 0.15%,0.2%, 0.4%) for 12 or 24 h. (**D**) RAW264.7 cells were treated with 0.05%, 0.1%, 0.15, and 0.2% CSE for 24 h. The mRNA levels of TNF-α in RAW264.7 cells were measured by RT-qPCR. (**E** and **F**) RAW264.7 cells were treated with 0.15% CSE for 0h, 6h, 12h, and 24 h. The protein and mRNA levels of TNF-α in RAW264.7 cells were measured. (**G**) C2C12 cells were co-cultured with RAW264.7 cells and then incubated with or without 0.15% CSE for 24 h. Representative microscopic images were taken. Black arrows indicate normal myotubes. Red arrows indicate cell death. Scale bar: 200 μm. (**H** and **I**) The protein levels of NLRP3, cleaved caspase-1, GSDMD-N, IL-1β, and IL-18 were measured in C2C12 cells co-cultured with RAW264.7 cells and incubated with or without CSE for 24 h. Data are expressed as the mean ± SD. Experiments were independently repeated three times with consistent results.

Notes: *P < 0.05, **P < 0.01, ***P < 0.001.

Abbreviation: ns: no significance.

https://doi.org/10.2147/JIR.S497631

To investigate the impact of macrophages on C2C12 cells, C2C12 myotubes were co-cultured with macrophages utilizing the Transwell system (Figure 2G). To determine the optimal concentration and incubation time, we added different concentrations of CSE to RAW264.7 cells. The activity of RAW264.7 cells was not affected after treatment with 0.05%, 0.1%, and 0.15% CSE for either 12 or 24 h (Figure 2C). RAW264.7 cells were stimulated with 0.05%, 0.1%, 0.15%, and 0.2% CSE for 24h, and the result indicated that the mRNA level of TNF-α in RAW264.7 cells was increased in the 0.15% CSE group and 0.2% CSE group compared with the control group. The stimulation effect of 0.15% CSE was stronger than that of the 0.2% CSE group (Figure 2D). Next, we stimulated macrophages with 0.15% CSE for 6 hours, 12 hours, and 24 hours to determine the time point for TNF-α expression. The results showed that both TNF-α mRNA and protein expression reached their peak levels at the 24-hour time point (Figure 2E and F). Hence, we treated RAW264.7 cells with 0.15% CSE for 24h in subsequent experiments. The results illustrated that C2C12 myotubes in the CSE group were swollen and necrotic in contrast to the control group (Figure 2G). Most importantly, pyroptosis-related indicators including NLRP3, GSDMD-N, cleaved caspase-1, IL-1β, and IL-18 had higher protein levels in C2C12 myotubes co-cultured with CSE-stimulated RAW264.7 cells than in the control group (Figure 2H and I). Meanwhile, the mRNA levels of GSDMD, Caspase-1, and NLRP3 were also upregulated in C2C12 myotubes from the CSE group (Figure 3A). In addition, CSE-activated macrophages promoted increased IL-1β release from C2C12 myotubes (Figure 3B). Finally, a significantly higher proportion of PI-positive C2C12 cells and a higher incidence of LDH release

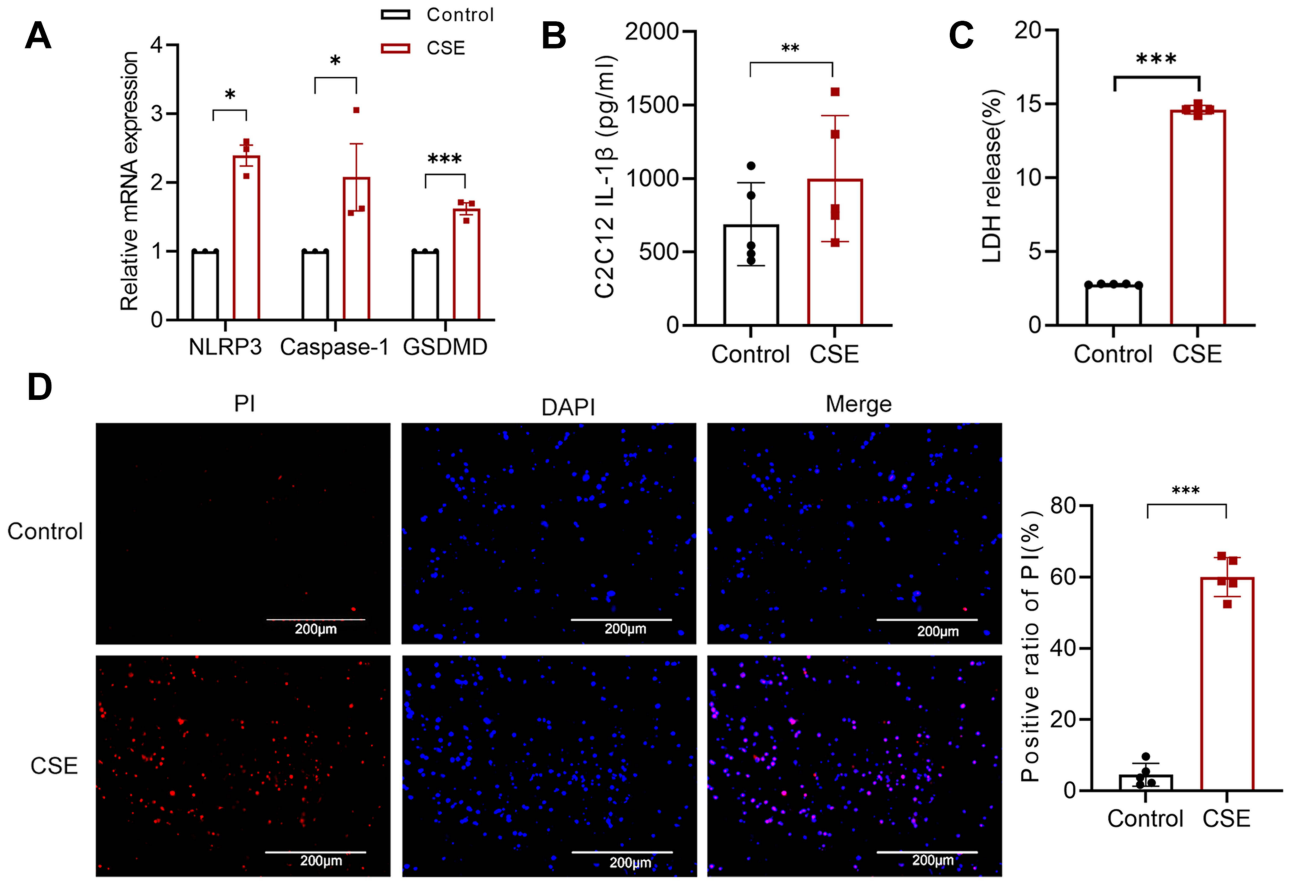

Figure 3 CSE-activated macrophages promote C2C12 myotubes pyroptosis. (**A**)The mRNA levels of NLRP3, caspase-1, and GSDMD were measured in C2C12 cells co-cultured with RAW264.7 cells and incubated with or without CSE for 24 h. (**B**) IL-1β levels in the supernatant of C2C12 cells co-cultured with RAW264.7 cells and incubated with or without CSE for 24 h. (**C**) LDH levels in the supernatant of C2C12 cells co-cultured with RAW264.7 cells and incubated with or without 0.15% CSE for 24 h. (**D**) Representative PI staining photographs of C2C12 myotubes co-cultured with RAW264.7 cells and incubated with or without 0.15% CSE for 24 h, and the PI positivity rate was quantified for each group. Scale bar: 200 μm. Data are expressed as the mean ± SD. Experiments were independently repeated three times with consistent results.
Notes: *$P < 0.05$, **$P < 0.01$, ***$P < 0.001$.
Abbreviation: ns: no significance.

were observed in the CSE group, suggesting that activated macrophages promote C2C12 cell death and extensive lysis (Figure 3C and D). These results suggest that CSE-activated macrophages promote C2C12 myotube pyroptosis.

Macrophage-Derived TNF-α Is an Initiator of Skeletal Muscle Pyroptosis

To investigate the mechanism by which CSE-stimulated macrophages promote enhanced skeletal muscle cell pyroptosis, we examined TNF-α secretion by RAW264.7 cells. Our findings indicated that CSE stimulated RAW264.7 cells to secret large amounts of TNF-α (Figure 4A). To study the function of TNF-α in this process, we utilized infliximab, a chimeric monoclonal antibody that inhibits TNF-α signaling. The results demonstrated that infliximab inhibited the the secretion of TNF-α by CSE-activated RAW264.7 cells (Figure 4B). Next, RAW264.7 cells were co-cultured with C2C12 cells after stimulation with CSE and treatment with or without 100 ng/mL infliximab for 2 h. The protein levels of NLRP3 and other pyroptosis-related factors, such as cleaved caspase-1, GSDMD-N, and IL-18, were higher in C2C12 cells incubated with CSE and TNF-α than those in the control group. Their protein levels in the CSE + infliximab group were lower than the CSE group (Figure 4C and D). Meanwhile, the CSE + infliximab group showed a decrease in both the NLRP3 mRNA level and the release of LDH in C2C12 myotubes related to the CSE group (Figure 4E and F). In addition, inhibition of TNF-α secretion by CSE-stimulated RAW264.7 cells mitigated the reduction in C2C12 myotube diameter triggered by CSE-activated macrophages (Figure 4G). These results suggest that the suppression of TNF-α release from CSE-activated macrophages attenuated pyroptosis and atrophy of C2C12 myotubes.

Knockdown of TNF-α in Macrophages Attenuates Skeletal Muscle Pyroptosis

To further validate the role of macrophage-secreted TNF-α in inducing pyroptosis in C2C12 myotubes, we knocked down TNF-α in RAW264.7 cells via lentiviral transfection. The efficacy of TNF-α knockdown was validated by Western blotting and RT-PCR, which confirmed substantial decreases in both TNF-α mRNA and protein level (Figure 5A and B). The successfully transfected RAW 264.7 cells displayed significantly lower TNF-α release after stimulation with CSE (Figure 5C and D). Following co-cultivation with C2C12 cells, the results indicated that NLRP3, caspase-1, GSDMD-N, IL-1β, and IL-18 mRNA and protein levels in C2C12 cells were all significantly lower in the shTNF-α + CSE group than in the shNC + CSE group (Figure 5E-H). ELISA demonstrated that IL-1β release from C2C12 cells was reduced in the shTNF-α + CSE group (Figure 5I). In addition, PI positivity in C2C12 myotubes was also significantly reduced in the shTNF-α + CSE group (Figure 5J and K).

CSE-activated macrophages promote skeletal muscle pyroptosis and atrophy through modulation of the TNF-α/TNFR1 signalling pathway

Previous studies revealed that TNF-α binds to TNFR1 to initiate complicated cell death signaling.[25] Our results indicated that TNFR1 protein expression was elevated in the GM of CS-exposed mice (Figure 6A). In the co-culture system, TNFR1 expression was elevated in C2C12 cells in the CSE group (Figure 6B and C). The addition of the anti-TNF-α antibody infliximab successfully reduced the increase in TNFR1 protein expression observed in C2C12 myotubes co-cultured with CSE-activated RAW264.7 cells (Figure 6D). C2C12 myotubes were also co-cultured with negative-control or TNF-α–depleted RAW 264.7 cells. Compared to shNC + CSE group, the mRNA and protein levels of TNFR1 was notably decreased in C2C12 myotubes in the shTNF-α + CSE group (Figure 6E and F).

To further demonstrate that TNF-α derived from macrophages induces pyroptosis through TNFR1, C2C12 myotubes were pretreated with or without the TNFR1-specific inhibitor R-7050 and then co-cultured with macrophages with or without CSE stimulation. The outcomes revealed that the expression of TNFR1 and pyroptosis-related proteins in C2C12 myotubes were markedly reduced by the addition of TNFR1 inhibitor R-7050 (Figure 6G and H). The rate of PI positivity and LDH release in C2C12 myotubes was also significantly reduced in the CSE +R-7050 group (Figure 6I and J, 7B). In addition, treatment with R-7050 reverse the reduction in myotube diameter induced by CSE-activated macrophages (Figure 6K and L). These results suggest that the CSE-activated macrophages promote skeletal muscle pyroptosis and atrophy via the TNF-α/TNFR1 pathway.

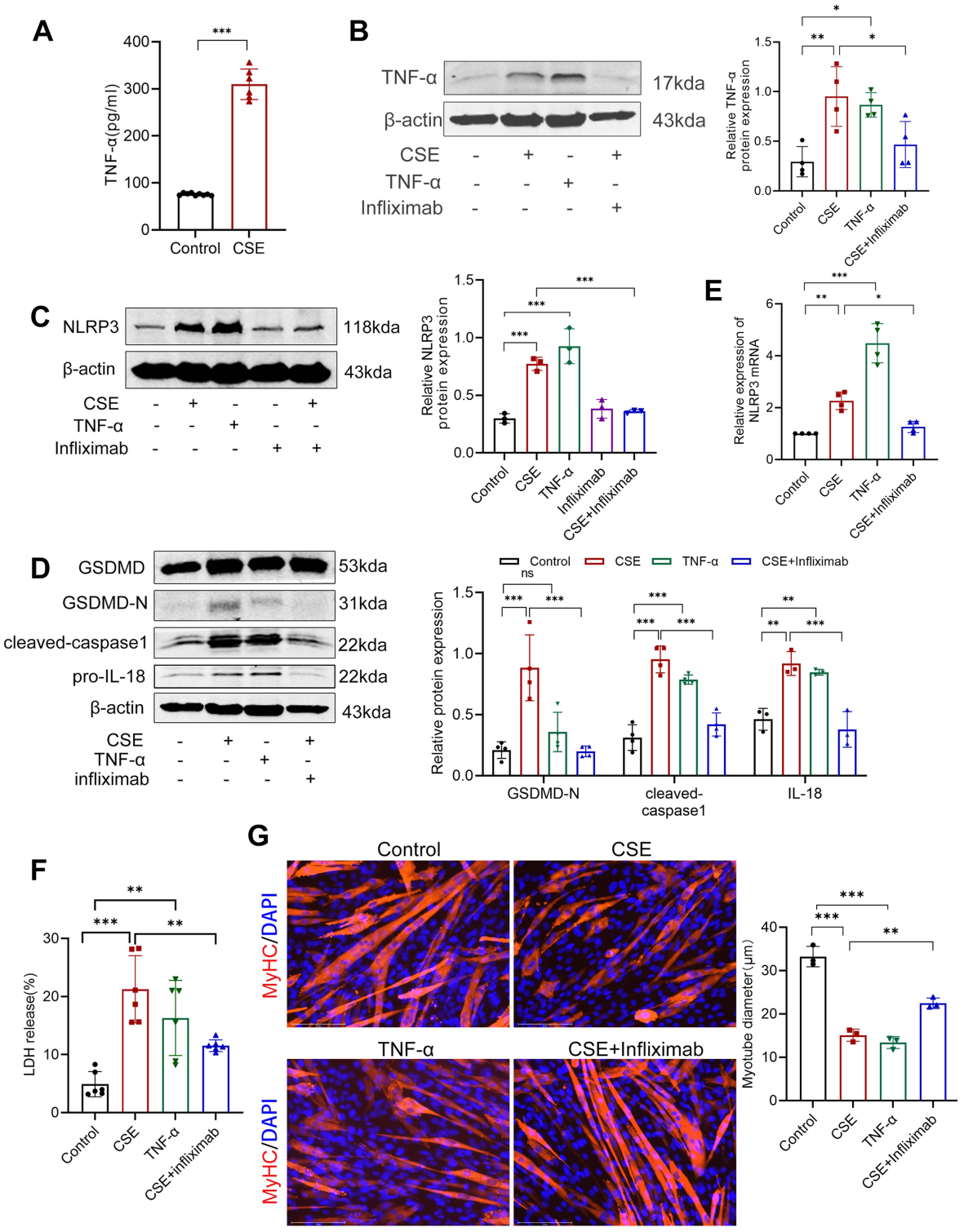

Figure 4 Macrophage-derived TNF-α is an initiator of skeletal muscle pyroptosis. RAW264.7 cells were incubated with CSE or 80 ng/mL TNF-α for 24 h and then treated with or without 100 ng/mL infliximab for 2 h. Then, RAW264.7 cells were co-cultured with C2C12 cells. (**A**) TNF-α levels were detected in the supernatant of RAW264.7 cells. (**B**) TNF-α protein expression in RAW264.7 cells measured by Western blotting. (**C**) NLRP3 protein expression was measured in C2C12 cells co-cultured with RAW264.7 cells (**D**) The protein levels of cleaved caspase-1, GSDMD-N, and pro-IL-18 were measured in C2C12 cells. (**E**) NLRP3 mRNA expression was measured in C2C12 cells. (**F**) RAW264.7 cells were incubated with CSE or 80 ng/mL TNF-α for 24 h and then treated with or without 100 ng/mL infliximab for 2 h. Then, RAW264.7 cells were co-cultured with C2C12 cells. LDH levels in the supernatant of C2C12 cells were examined. (**G**) Immunofluorescence staining for MyHC (red)/nuclei (blue) were examined in C2C12 myotubes between the four groups. The distribution of the C2C12 myotube diameter was analyzed. Scale bar: 125 μm.

Notes: *P < 0.05, **P < 0.01, ***P < 0.001.

Abbreviation: ns: no significance.

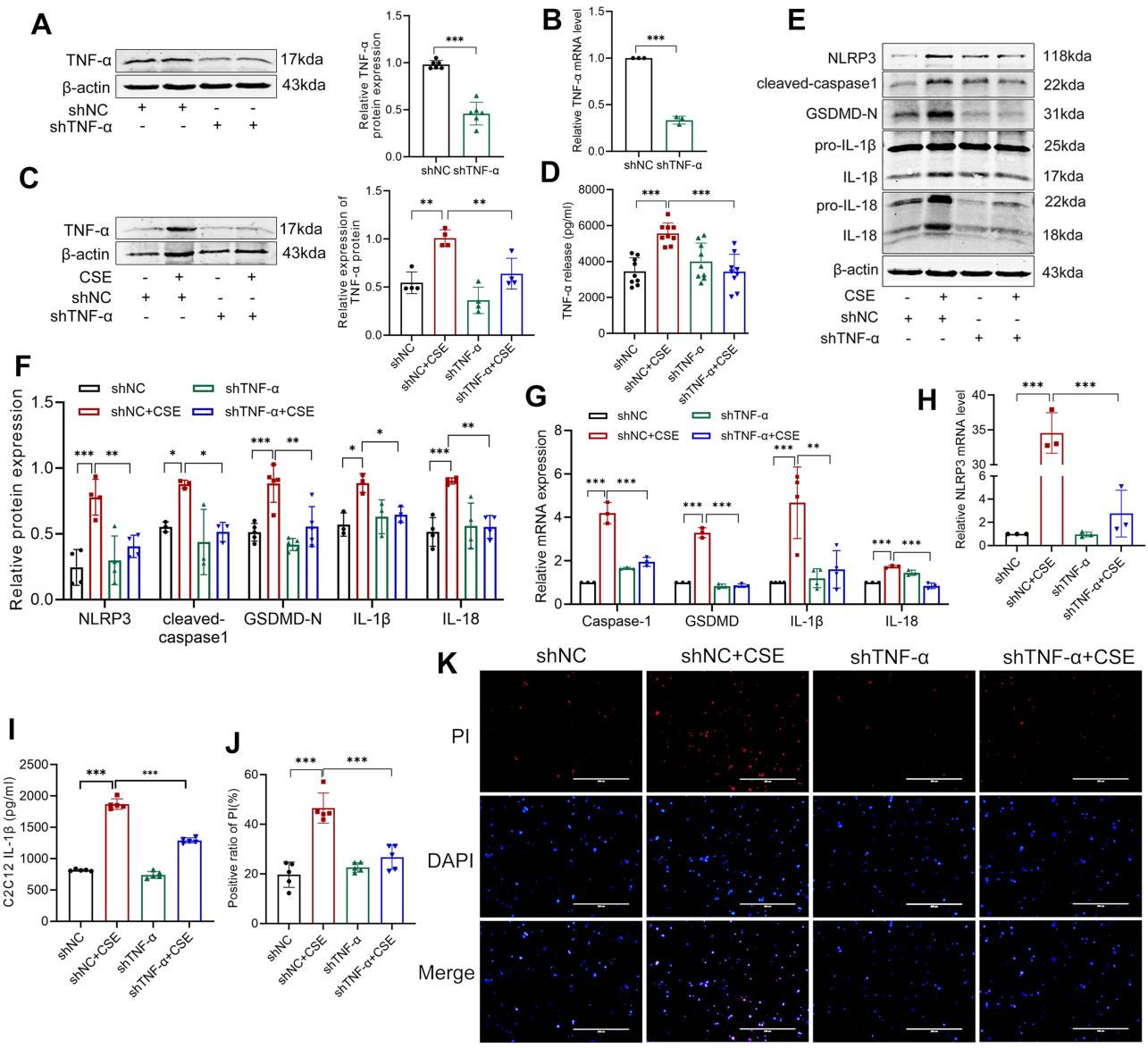

Figure 5 Knockdown of TNF-α in macrophages attenuates skeletal muscle pyroptosis. (**A**) The effect of TNF-α knockdown on TNF-α protein expression in RAW264.7 cells as determined by Western blotting. (**B**) The effect of TNF-α knockdown on TNF-α mRNA expression in RAW264.7 cells as measured by RT-PCR. (**C**) TNF-α protein expression in negative-control or TNF-α–depleted RAW264.7 cells treated with or without CSE for 24 h. (**D**) Negative-control or TNF-α–depleted RAW264.7 cells were co-cultured with C2C12 cells and then treated with or without CSE for 24 h. TNF-α levels in the supernatant of RAW264.7 cells as determined by ELISA. (**E** and **F**) Negative-control or TNF-α–depleted RAW264.7 cells were co-cultured with C2C12 cells and then treated with or without CSE for 24 h. The protein levels of NLRP3, cleaved caspase-1, GSDMD-N, IL-1β, and IL-18 in C2C12 cells. (**G** and **H**) The mRNA levels of NLRP3, caspase-1, GSDMD, IL-1β, and IL-18 in C2C12 cells. (**I**) IL-1β levels were detected in the supernatant of C2C12 cells by ELISA. (**J** and **K**) Representative PI staining photographs of C2C12 cells co-cultured with negative-control or TNF-α–depleted RAW264.7 cells after treating co-cultured cells with or without CSE. PI positivity rate among C2C12 cells was measured for each group. Scale bar: 200 μm.
Notes: *P < 0.05, **P < 0.01, ***P < 0.001.
Abbreviations: ns: no significance,shNC, negative control; shTNF-α, TNF-α knockdown.

NLRP3 Inflammasome Is Required for Skeletal Muscle Pyroptosis Induced by CSE-Activated Macrophages

The NLRP3 inflammasome is an upstream signal that regulates pyroptosis. To confirm the function of NLRP3 in activated macrophages-induced pyroptosis, C2C12 myotubes were pretreated with NLRP3-specific inhibitor MCC950 and then co-cultured with RAW264.7 macrophages with or without CSE stimulation. In C2C12 cells, the expression of NLRP3 and other pyroptosis-related factors was diminished in the CSE + MCC950 relative to the CSE group (Figure 7A, C, and D). In addition, LDH release and PI positivity in C2C12 myotubes were also reduced in the CSE + MCC950 group (Figure 7B and E).

https://doi.org/10.2147/JIR.S497631

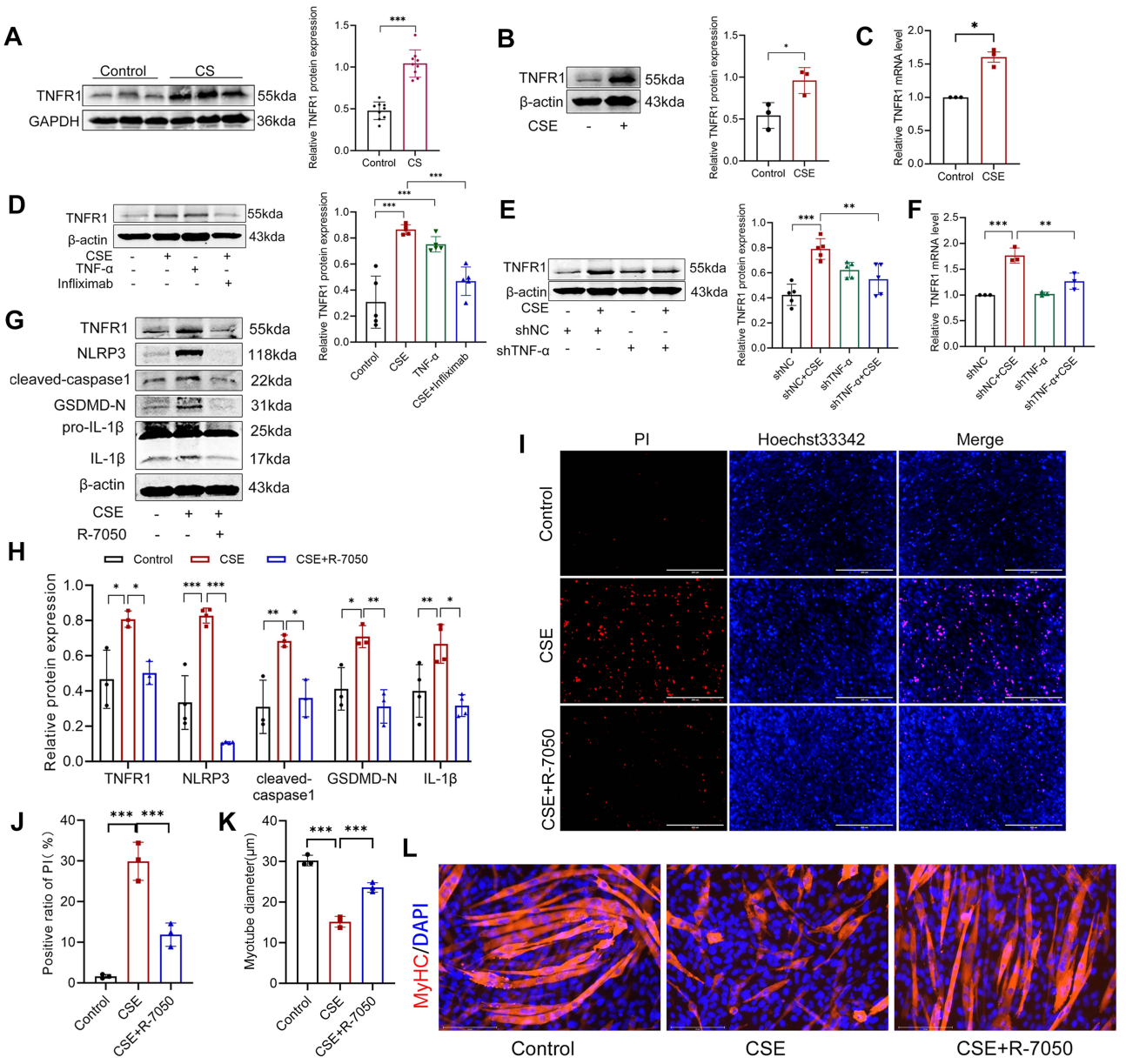

Figure 6 CSE-activated macrophages promote skeletal muscle pyroptosis through modulation of the TNF-α/TNFR1 signalling pathway. (**A**) TNFR1 protein expression was measured in the GM tissue of mice exposed to room air or CS for 24 weeks. (**B**) C2C12 cells were co-cultured with RAW264.7 cells and then incubated with or without CSE for 24 h. TNFR1 protein expression was measured in C2C12 cells. (**C**) TNFR1 mRNA levels were measured in C2C12 cells co-cultured with RAW264.7 cells treated with or without CSE. (**D**) RAW264.7 cells were incubated with CSE or 80 ng/mL TNF-α for 24 h and then treated with or without 100 ng/mL infliximab for 2 h. Then, RAW264.7 cells were co-cultured with C2C12 cells. TNFR1 protein expression was measured in C2C12 cells. (**E**) TNFR1 protein expression was measured in C2C12 cells after co-culture with negative-control or TNF-α–depleted RAW264.7 cells incubated with or without CSE. (**F**) TNFR1 mRNA levels were measured in C2C12 cells after co-culture with negative-control or TNF-α–depleted RAW264.7 cells incubated with or without CSE. (**G** and **H**) C2C12 cells were pretreated with or without 5 μM R-7050 for 2 h and then co-cultured with RAW264.7 cells with or without CSE stimulation. Protein expression of TNFR1, NLRP3, cleaved caspase-1, GSDMD-N, and IL-1β was detected in C2C12 cells. (**I** and **J**) Representative Hoechst/PI staining photographs of C2C12 cells pretreated with or without 5 μM R-7050 for 2 h and then co-cultured with RAW264.7 cells with or without CSE stimulation, and the PI positivity rate was quantified for each group. Scale bar: 200 μm. (**K** and **L**) Immunofluorescence staining for MyHC (red) in C2C12 myotubes. Nuclei were stained with DAPI (blue). The distribution of the C2C12 myotube diameter was analyzed. Scale bar: 125 μm.
Notes: **P* < 0.05, ***P* < 0.01, ****P* < 0.001.
Abbreviation: ns: no significance.

Furthermore, treatment with MCC950 mitigated the CSE-activated macrophage-induced reduction in C2C12 myotube diameter (Figure 7F). These results suggest that CSE-activated macrophages promote skeletal muscle atrophy and pyroptosis, which requires the NLRP3 inflammasome.

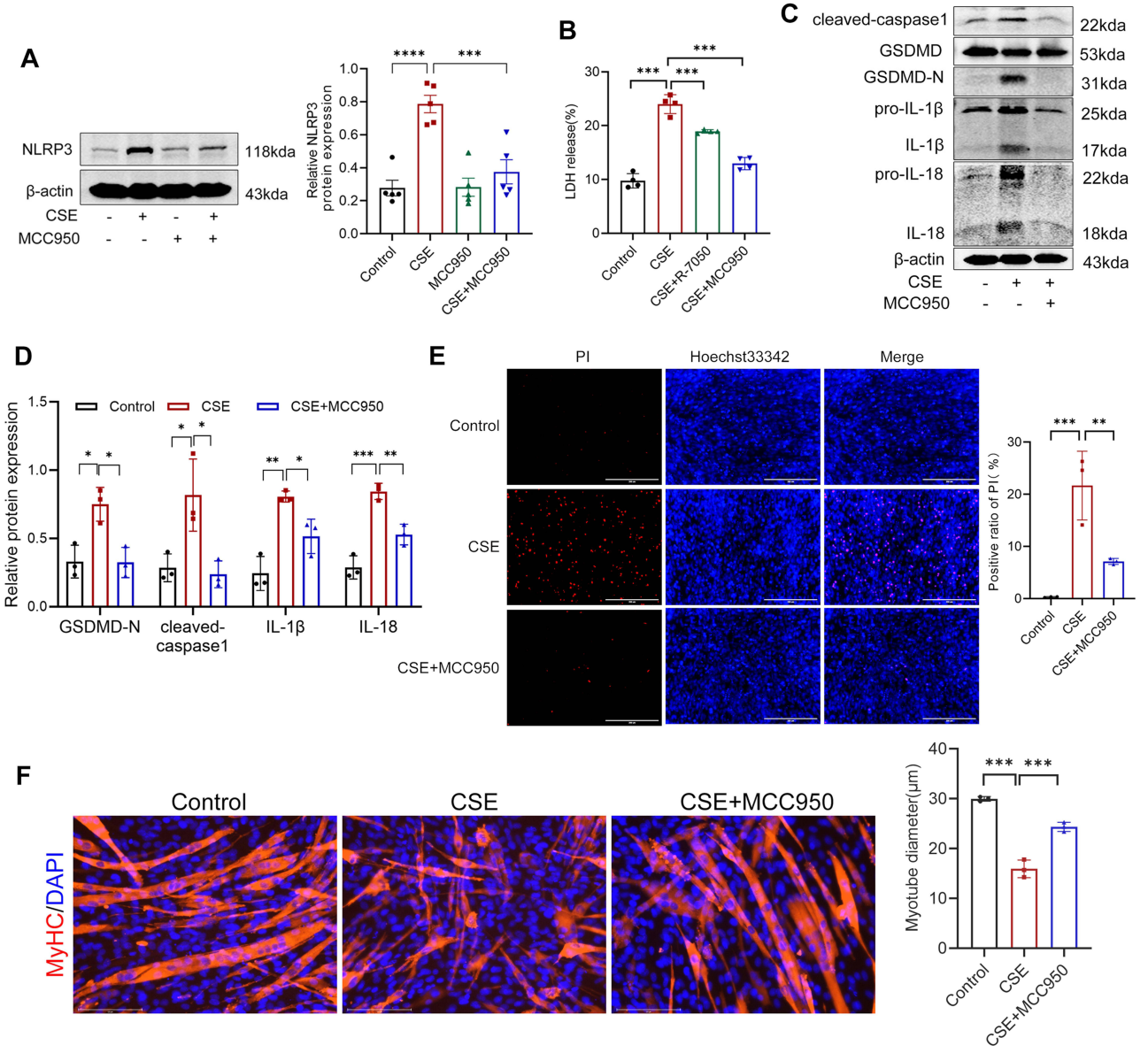

Figure 7 NLRP3 inflammasome is required for skeletal muscle pyroptosis induced by CSE-activated macrophages. C2C12 myotubes pretreated with or without 5 μM MCC950 for 1 h and then co-cultured with RAW264.7 cells with or without CSE stimulation. (**A**) NLRP3 protein expression in C2C12 myotubes was measured by Western blotting. (**B**) C2C12 cells were pretreated with or without 5 μM R-7050 or 5 μM MCC950 for 1 h and then co-cultured with RAW264.7 cells with or without CSE stimulation. LDH levels were measured in the supernatant of C2C12 cells. (**C** and **D**) Protein expression of cleaved caspase-1, GSDMD-N, IL-1β, and IL-18 in C2C12 myotubes was measured by Western blotting. (**E**) Representative Hoechst/PI staining photographs of C2C12 cells, and the PI positivity rate was quantified for each group. Scale bar: 200 μm. (**F**) Immunofluorescence staining for MyHC (red) in C2C12 myotubes. Nuclei were stained with DAPI (blue). The distribution of the C2C12 myotube diameter was analyzed. Scale bar: 125 μm.

Notes: **P* < 0.05, ***P* < 0.01, ****P* < 0.001.

Abbreviation: ns: no significance.

Discussion

Macrophages play crucial roles in skeletal muscle injury and repair processes.[26] However, their specific roles and the underlying interactions within the context of skeletal muscle atrophy induced by oxidative stress following CS exposure remain to be elucidated. This research explored the impact of macrophages on CS-induced skeletal muscle atrophy. Investigations using a murine COPD mode revealed that CS exposure contributed to GM atrophy and increased pyroptosis. In addition, we found that TNF-α secreted by CSE-activated macrophages promoted pyroptosis in C2C12 myotubes, which in turn induced skeletal muscle

https://doi.org/10.2147/JIR.S497631

atrophy. Further investigations demonstrated that TNF-α secreted from CSE-activated macrophages induced skeletal muscle pyroptosis through the TNFR1/NLRP3/caspase-1/GSDMD/IL-18/IL-1β pathways.

Previous studies have explored the mechanisms underlying muscle atrophy in COPD. These studies mainly focused on the mechanisms of systemic inflammatory response, oxidative stress, imbalance in protein synthesis and catabolism, mitochondrial dysfunction, hypoxia and hypercapnia, decreased activity, malnutrition, and other factors.[27–29] Additionally, the ubiquitin proteasome system (UPS) and autophagy have also been identified to contribute to skeletal muscle atrophy.[30] However, skeletal muscle atrophy in COPD may be caused by multiple molecular mechanisms. Pyroptosis may be another potential mechanism of skeletal muscle atrophy associated with COPD. Our research revealed that prolonged exposure to CS results in GM atrophy and decreases in muscle fiber differentiation capacity in mice, as evidenced by decreases in body weight, GM weight, muscle fiber CSA, and muscle specific gene expression in mice. Meanwhile, CS induces increased expression of pyroptosis-associated molecules, including NLRP3, cleaved caspase-1, GSDMD-N, and IL-18. CS-induced GM atrophy is accompanied by increased pyroptosis. There is increasing evidence indicating that sterile oxidative stress-induced pyroptosis promotes skeletal muscle atrophy,[31] suggesting that pyroptosis induced by CS exposure may be a significant factor in skeletal muscle atrophy in mice with COPD.

Pyroptosis can be triggered by the recognition of various molecular patterns, including DAMPs, PAMPs, and the cytokine TNF-α.[32] In this study, CS increased TNF-α expression in the GM of mice. TNF-α limits cell differentiation events and leads to muscle wasting.[33] Inhibition of TNF-α signaling diminishes tissue breakdown associated with TNF-α and facilitates the constructive remodeling of skeletal muscles following injuries.[34] Previous studies confirmed that TNF-α–mediated pyroptosis promotes skeletal muscle atrophy in aged mice.[35] In this study, TNF-α induced C2C12 myotube atrophy accompanied by an increase in pyroptosis, suggesting that TNF-α induces skeletal muscle atrophy in COPD, likely through enhanced pyroptosis.

The origin of TNF-α has consistently been a central focus of research. CS can directly stimulate TNF-α production in skeletal muscle cells.[36] However, our previous research found that inhibiting TNF-α induced by CS in C2C12 cells does not reverse skeletal muscle atrophy.[16] This suggests that additional sources of TNF-α are involved in the development of skeletal muscle wasting associated with COPD. TNF-α is primarily produced by macrophages.[37,38] Recent studies identified a mixed population of self-renewing and non-self-renewing resident macrophages in skeletal muscle.[39] Non-resident macrophages are derived from blood monocytes, and they migrate into tissues in response to damage or infection.[40] The substantial release of TNF-α from skeletal muscle-resident macrophages, circulating activated macrophages, or alveolar macrophages might promote skeletal muscle pyroptosis through a spillover effect.[41] Prior research demonstrated that CS exposure resulted in skeletal muscle dysfunction and increased macrophage infiltration into the injured muscle tissue, which could be another factor contributing to the reduction in muscle regenerative capacity.[13] Macrophages in local tissues might also exert an effect in a paracrine manner. Therefore, the interaction between macrophages and skeletal muscle cells in the context of CS exposure warrants further investigation.

In this study, CSE-activated macrophages induced swelling and necrosis of C2C12 myotubes. Furthermore, CSE-activated macrophages increased the expression of pyroptosis-related molecules and the release of IL-1β in C2C12 myotubes. Additionally, the release of TNF-α from CSE-activated macrophages was also increased. These findings suggest that CSE-activated macrophages promote enhanced pyroptosis in C2C12 myotubes, possibly related to TNF-α released by activated macrophages.

To further investigate the role of TNF-α derived from macrophages in skeletal muscle cell pyroptosis, we knocked down the TNF-α gene in macrophages. Our results illustrated that TNF-α knockdown reverses CSE-activated macrophage-induced enhancement of C2C12 myotube pyroptosis. Comparable outcomes were observed in C2C12 cells co-cultured with macrophages treated with TNF-α inhibitors. In addition, inhibition of TNF-α secreted from CSE-stimulated macrophages attenuated C2C12 myotube atrophy. These results further confirmed that TNF-α secreted from CSE-activated macrophages enhances pyroptosis and in turn promotes skeletal muscle atrophy. However, CSE significantly enhances the expression of GSDMD in cells more than TNF-α alone, indicating that other inflammatory factors other than TNF-α may influence GSDMD expression and contribute to the reduction in myotube diameter through distinct mechanisms. Studies have shown that CSE can stimulate the release of a range of inflammatory factors in skeletal muscle cells, such as IL-8 and IL-6.[16] CSE induces the overproduction of IL-8 in lungs and its release into the circulation, a process which has been linked to the occurrence of skeletal muscle atrophy.[42] IL-6 is highly expressed in COPD and is considered a biomarker of systemic inflammation and has also been associated with sarcopenia. IL-6 activates the JAK/

STAT pathway and PI3K/AKT/mTOR pathway by binding to its receptors,[43,44] thereby promoting the reduction of protein synthesis and the increase of protein degradation in skeletal muscle tissue.

Previous studies demonstrated that the binding of TNF-α to TNFR1 contributes to muscle weakness.[45,46] The TNF-α/TNFR1 pathway participates in numerous biological processes and is crucial in various disorders, including skin necroptotic inflammation.[47] However, it remains unclear whether TNF-α released by CSE-activated macrophages promotes pyroptosis through TNFR1 activation in C2C12 cells. In this investigation, TNFR1 protein expression was increased in the GM of mice exposed to CS and in C2C12 myotubes co-cultured alongside CSE-activated macrophages or with recombinant TNF-α. Subsequent inhibition or knockdown of TNF-α in macrophages effectively reversed the CSE-induced elevation of TNFR1 expression in C2C12 myotubes. These findings suggest that TNF-α from activated macrophages likely promotes pyroptosis in C2C12 myotubes through binding to TNFR1. Moreover, Inhibition of TNFR1 in C2C12 myotubes effectively reversed the enhanced myotube pyroptosis and atrophy induced by CSE-activated macrophages. These findings suggest that CSE-activated macrophages may induce skeletal muscle pyroptosis and atrophy through the TNF-α/TNFR1 pathway.

Activation of NLRP3 inflammasome has been observed in skeletal muscle in various models of muscle wasting.[48–50] NLRP3 serves as an upstream regulator of cellular pyroptosis, and it can be activated by various extracellular signaling molecules, such as TNF-α.[51] Previous studies have shown that CS activates the NLRP3 inflammasome through multiple pathways, promoting pyroptosis in various tissues and cells, thereby contributing to the development of a numerous diseases. Additional studies have shown that CSE induces pyroptosis and inflammation in human bronchial epithelial cells via the ROS/NLRP3/caspase-1 pathway.[52] CS exposure mediates the activation of NLRP3 inflammasome through the sGC/cGMP/PKG/TACE/TNF-α pathway, leading to aortic endothelial cell pyroptosis and vascular dysfunction.[53] In pancreatic islet β cells, studies have also shown that CS mediates increased inflammation and pyroptosis through the TXNIP-NLRP3-GSDMD axis, leading to hyperglycemia.[54] Consequently, activation of NLRP3 inflammasome might be a crucial mechanism through which TNF-α secreted from CSE-activated macrophages enhances myotubes pyroptosis. Our data indicated that NLRP3 expression was increased within the muscular tissue of mice exposed to CS and in C2C12 myotubes co-cultured alongside CSE-activated macrophages. TNF-α is a significant transcriptional regulator of the NLRP3 inflammasome.[34] In this study, TNF-α inhibition or knockdown in macrophages effectively reversed the CSE-induced increase in NLRP3 levels in C2C12 myotubes. Inhibition of NLRP3 in C2C12 myotubes also effectively reversed the enhanced myotube pyroptosis and atrophy induced by CSE-activated macrophages. These findings support that CSE-activated macrophages induce skeletal muscle pyroptosis by activating the NLRP3 inflammasome.

Limitations

Our study did not validate the therapeutic effect of targeting TNF-α–mediated pyroptosis in vivo using a murine COPD model featuring TNF-α knockdown or by administering an anti-TNF-α antibody to mice. Additionally, we have not yet investigated other factors secreted by macrophages that could potentially play a role in regulating pyroptosis in skeletal muscle cells and their downstream signaling. We will continue our efforts to conduct further studies on these topics.

Conclusion

Our research demonstrated that macrophage infiltration may be involved in the CS-induced skeletal muscle atrophy. Under the stimulation of CSE, TNF-α released by macrophages can promote the increase of pyroptosis in the skeletal muscle cells, which likely contributes to skeletal muscle atrophy. This process appears to be mediated through the TNFR1/NLRP3/Caspase-1/GSDMD signaling pathway. Therefore, investigating the interaction of these macrophage-secreted inflammatory mediators with skeletal muscle can provide more insight into the mechanisms underlying skeletal muscle atrophy in COPD.

Ethics Approval and Consent to Participate

All animal experiments were approved by the Guangxi Medical University Laboratory Animal Committee and conducted per the requirements of the Animal Care and Use Committee (Approval NO. 202401008).

Author Contributions

All authors made a significant contribution to the work reported, whether that is in the conception, study design, execution, acquisition of data, analysis and interpretation, or in all these areas; took part in drafting, revising or critically reviewing the article; gave final approval of the version to be published; have agreed on the journal to which the article has been submitted; and agree to be accountable for all aspects of the work.

Funding

This work was supported by the Joint Project on Regional High-Incidence Diseases Research of the Guangxi Natural Science Foundation under grant No. 2023GXNSFAA026303, the Cultivation Science Foundation of The Second Affiliated Hospital of Guangxi Medical University (grant number: GJPY2023010), and Guangxi University of Chinese Medicine University-level Scientific Research Youth Project (2022QN009).

Disclosure

The authors declare no conflicts of interest in this work.

References

1. Halpin DMG, Criner GJ, Papi A. et al. Global initiative for the diagnosis, management, and prevention of chronic obstructive lung disease. The 2020 GOLD science committee report on COVID-19 and chronic obstructive pulmonary disease. *Am J Respir Crit Care Med*. 2021;203(1):24–36. doi:10.1164/rccm.202009-3533SO
2. Sepúlveda-Loyola W, Osadnik C, Phu S, Morita AA, Duque G, Probst VS. Diagnosis, prevalence, and clinical impact of sarcopenia in COPD: a systematic review and meta-analysis. *J Cachexia, Sarcopenia Muscle*. 2020;11(5):1164–1176. doi:10.1002/jcsm.12600
3. Barnes PJ. Senescence in COPD and Its Comorbidities. *Annu Rev Physiol*. 2017;79(1):517–539. doi:10.1146/annurev-physiol-022516-034314
4. Nowiński A, Kamiński D, Korzybski D, Stokłosa A, Górecka D. The impact of comorbidities on the length of hospital treatment in patients with chronic obstructive pulmonary disease. *Pneumonol Alergol Pol*. 2011;79(6):388–396.
5. Schols AM, Slangen J, Volovics L, Wouters EF. Weight loss is a reversible factor in the prognosis of chronic obstructive pulmonary disease. *Am J Respir Crit Care Med*. 1998;157(6 Pt 1):1791–1797. doi:10.1164/ajrccm.157.6.9705017
6. Swallow EB, Reyes D, Hopkinson NS, et al. Quadriceps strength predicts mortality in patients with moderate to severe chronic obstructive pulmonary disease. *Thorax*. 2007;62(2):115–120. doi:10.1136/thx.2006.062026
7. Erratum. Skeletal muscle dysfunction in chronic obstructive pulmonary disease: what we know and can do for our patients. *Am J Respir Crit Care Med*. 2018;198(6):824–825. doi:10.1164/rccm.v198erratum3.
8. Degens H, Gayan-Ramirez G, van Hees HWH. Smoking-induced skeletal muscle dysfunction: from evidence to mechanisms. *Am J Respir Crit Care Med*. 2015;191(6):620–625. doi:10.1164/rccm.201410-1830PP
9. Hernández-Hernández JM, García-González EG, Brun CE, Rudnicki MA. The myogenic regulatory factors, determinants of muscle development, cell identity and regeneration. *Semin Cell Dev Biol*. 2017;72:10–18. doi:10.1016/j.semcdb.2017.11.010
10. Peterson JM, Bryner RW, Alway SE. Satellite cell proliferation is reduced in muscles of obese Zucker rats but restored with loading. *Am J Physiol Cell Physiol*. 2008;295(2):C521–528. doi:10.1152/ajpcell.00073.2008
11. Haas GJ, Dunn AJ, Marcinczyk M, et al. Biomimetic sponges for regeneration of skeletal muscle following trauma. *J Biomed Mater Res A*. 2019;107(1):92–103. doi:10.1002/jbm.a.36535
12. Barnes PJ, Celli BR. Systemic manifestations and comorbidities of COPD. *Eur Respir J*. 2009;33(5):1165–1185. doi:10.1183/09031936.00128008
13. Chan SMH, Cerni C, Passey S, et al. Cigare tte smoking exacerbates skeletal muscle injury without compromising its regenerative capacity. *Am J Respir Cell mol Biol*. 2020;62(2):217–230. doi:10.1165/rcmb.2019-0106OC
14. Pascual-Fernández J, Fernández-Montero A, Córdova-Martínez A, Pastor D, Martínez-Rodríguez A, Roche E. Sarcopenia: molecular pathways and potential targets for intervention. *Int J mol Sci*. 2020;21(22):8844. doi:10.3390/ijms21228844
15. Sishi BJN, Engelbrecht AM. Tumor necrosis factor alpha (TNF-α) inactivates the PI3-kinase/PKB pathway and induces atrophy and apoptosis in L6 myotubes. *Cytokine*. 2011;54(2):173–184. doi:10.1016/j.cyto.2011.01.009
16. Bin Y, Xiao Y, Huang D, et al. Theophylline inhibits cigarette smoke-induced inflammation in skeletal muscle by upregulating HDAC2 expression and decreasing NF-κB activation. *Am J Physiol Lung Cell mol Physiol*. 2019;316(1):L197–L205. doi:10.1152/ajplung.00005.2018
17. Liu D, Xiao Y, Zhou B, et al. PKM2-dependent glycolysis promotes skeletal muscle cell pyroptosis by activating the NLRP3 inflammasome in dermatomyositis/polymyositis. *Rheumatology (Oxford)*. 2021;60(5):2177–2189. doi:10.1093/rheumatology/keaa473
18. Aluganti Narasimhulu C, Singla DK. Amelioration of diabetes-induced inflammation mediated pyroptosis, sarcopenia, and adverse muscle remodelling by bone morphogenetic protein-7. *J Cachexia, Sarcopenia Muscle*. 2021;12(2):403–420. doi:10.1002/jcsm.12662
19. Zhang L, Li C, Xiong J, Chang C, Sun Y. Dysregulated myokines and signaling pathways in skeletal muscle dysfunction in a cigarette smoke-induced model of chronic obstructive pulmonary disease. *Front Physiol*. 2022;13:929926. doi:10.3389/fphys.2022.929926
20. Dubuisson N, Versele R, Davis-López de Carrizosa MA, Selvais CM, Brichard SM, Abou-Samra M. Walking down skeletal muscle lane: from inflammasome to disease. *Cells*. 2021;10(11):3023. doi:10.3390/cells10113023
21. McGeough MD, Wree A, Inzaugarat ME, et al. TNF regulates transcription of NLRP3 inflammasome components and inflammatory molecules in cryopyrinopathies. *J Clin Invest*. 2017;127(12):4488–4497. doi:10.1172/JCI90699
22. Zhang N, Zhang J, Yang Y, et al. A palmitoylation-depalmitoylation relay spatiotemporally controls GSDMD activation in pyroptosis. *Nat Cell Biol*. 2024;26(5):757–769. doi:10.1038/s41556-024-01397-9

23. Kang MJ, Shadel GS. A mitochondrial perspective of chronic obstructive pulmonary disease pathogenesis. *Tuberc Respir Dis (Seoul)*. 2016;79(4):207–213. doi:10.4046/trd.2016.79.4.207
24. Fan X, Dong T, Yan K, Ci X, Peng L. PM2.5 increases susceptibility to acute exacerbation of COPD via NOX4/Nrf2 redox imbalance-mediated mitophagy. *Redox Biol*. 2022;59:102587. doi:10.1016/j.redox.2022.102587
25. Wajant H, Scheurich P. TNFR1-induced activation of the classical NF-κB pathway. *FEBS J*. 2011;278(6):862–876. doi:10.1111/j.1742-4658.2011.08015.x
26. Henrot P, Blervaque L, Dupin I, et al. Cellular interplay in skeletal muscle regeneration and wasting: insights from animal models. *J Cachexia, Sarcopenia Muscle*. 2023;14(2):745–757. doi:10.1002/jcsm.13103
27. Doucet M, Russell AP, Léger B, et al. Muscle atrophy and hypertrophy signaling in patients with chronic obstructive pulmonary disease. *Am J Respir Crit Care Med*. 2007;176(3):261–269. doi:10.1164/rccm.200605-704OC
28. Langen RCJ, Gosker HR, Remels AHV, Schols AMWJ. Triggers and mechanisms of skeletal muscle wasting in chronic obstructive pulmonary disease. *Int J Biochem Cell Biol*. 2013;45(10):2245–2256. doi:10.1016/j.biocel.2013.06.015
29. Xiong J, Le Y, Rao Y, et al. RANKL mediates muscle atrophy and dysfunction in a cigarette smoke-induced model of chronic obstructive pulmonary disease. *Am J Respir Cell mol Biol*. 2021;64(5):617–628. doi:10.1165/rcmb.2020-0449OC
30. Yoshida T, Delafontaine P. Mechanisms of IGF-1-mediated regulation of skeletal muscle hypertrophy and atrophy. *Cells*. 2020;9(9):1970. doi:10.3390/cells9091970
31. Narasimhulu CA, Singla DK. BMP-7 attenuates sarcopenia and adverse muscle remodeling in diabetic mice via alleviation of lipids, inflammation, HMGB1, and pyroptosis. *Antioxidants (Basel)*. 2023;12(2):331. doi:10.3390/antiox12020331
32. Wen J, Xuan B, Liu Y, et al. NLRP3 inflammasome-induced pyroptosis in digestive system tumors. *Front Immunol*. 2023;14:1074606. doi:10.3389/fimmu.2023.1074606
33. Reid MB, Li YP. Tumor necrosis factor-α and muscle wasting: a cellular perspective. *Respir Res*. 2001;2(5):269. doi:10.1186/rr67
34. Stratos I, Behrendt AK, Anselm C, Gonzalez A, Mittlmeier T, Vollmar B. Inhibition of TNF-α restores muscle force, inhibits inflammation, and reduces apoptosis of traumatized skeletal muscles. *Cells*. 2022;11(15):2397. doi:10.3390/cells11152397
35. Wu J, Lin S, Chen W, et al. TNF-α contributes to sarcopenia through caspase-8/caspase-3/GSDME-mediated pyroptosis. *Cell Death Discov*. 2023;9(1):76. doi:10.1038/s41420-023-01365-6
36. De Paepe B, Brusselle GG, Maes T, et al. TNF alpha receptor genotype influences smoking-induced muscle-fibre-type shift and atrophy in mice. *Acta Neuropathol*. 2008;115(6):675–681. doi:10.1007/s00401-008-0348-4
37. Libert C. Cytokine anniversary: TNF trailblazers five centuries apart. *Nature*. 2015;523(7559):158. doi:10.1038/523158e
38. Barnes PJ. Inflammatory mechanisms in patients with chronic obstructive pulmonary disease. *J Allergy Clin Immunol*. 2016;138(1):16–27. doi:10.1016/j.jaci.2016.05.011
39. Bian Z, Gong Y, Huang T, et al. Deciphering human macrophage development at single-cell resolution. *Nature*. 2020;582(7813):571–576. doi:10.1038/s41586-020-2316-7
40. Lazarov T, Juarez-Carreño S, Cox N, Geissmann F. Physiology and diseases of tissue-resident macrophages. *Nature*. 2023;618(7966):698–707. doi:10.1038/s41586-023-06002-x
41. Lee JH, Hailey KL, Vitorino SA, Jennings PA, Bigby TD, Breen EC. Cigarette smoke triggers IL-33-associated inflammation in a model of late-stage chronic obstructive pulmonary disease. *Am J Respir Cell mol Biol*. 2019;61(5):567–574. doi:10.1165/rcmb.2018-0402OC
42. Callaway CS, Delitto AE, D'Lugos AC, et al. IL-8 released from human pancreatic cancer and tumor-associated stromal cells signals through a CXCR2-ERK1/2 axis to induce muscle atrophy. *Cancers (Basel)*. 2019;11(12):1863. doi:10.3390/cancers11121863
43. Gao S, Durstine JL, Koh HJ, Carver WE, Frizzell N, Carson JA. Acute myotube protein synthesis regulation by IL-6-related cytokines. *Am J Physiol Cell Physiol*. 2017;313(5):C487–C500. doi:10.1152/ajpcell.00112.2017
44. Hirata Y, Nomura K, Kato D, et al. A Piezo1/KLF15/IL-6 axis mediates immobilization-induced muscle atrophy. *J Clin Invest*. 2022;132(10):e154611. doi:10.1172/JCI154611
45. Reid MB, Moylan JS. Beyond atrophy: redox mechanisms of muscle dysfunction in chronic inflammatory disease. *J Physiol*. 2011;589(Pt 9):2171–2179. doi:10.1113/jphysiol.2010.203356
46. Llovera M, García-Martínez C, López-Soriano J, et al. Protein turnover in skeletal muscle of tumour-bearing transgenic mice overexpressing the soluble TNF receptor-1. *Cancer Lett*. 1998;130(1–2):19–27. doi:10.1016/s0304-3835(98)00137-2
47. Nam YW, Shin JH, Kim S, et al. EGFR inhibits TNF-α-mediated pathway by phosphorylating TNFR1 at tyrosine 360 and 401. *Cell Death Differ*. 2024. doi:10.1038/s41418-024-01316-3
48. Irazoki A, Martinez-Vicente M, Aparicio P, et al. Coordination of mitochondrial and lysosomal homeostasis mitigates inflammation and muscle atrophy during aging. *Aging Cell*. 2022;21(4):e13583. doi:10.1111/acel.13583
49. McBride MJ, Foley KP, D'Souza DM, et al. The NLRP3 inflammasome contributes to sarcopenia and lower muscle glycolytic potential in old mice. *Am J Physiol Endocrinol Metab*. 2017;313(2):E222–E232. doi:10.1152/ajpendo.00060.2017
50. Antuña E, Potes Y, Baena-Huerta FJ, et al. NLRP3 contributes to sarcopenia associated to dependency recapitulating inflammatory-associated muscle degeneration. *Int J mol Sci*. 2024;25(3):1439. doi:10.3390/ijms25031439
51. Wang L, Jiao XF, Wu C, et al. Trimetazidine attenuates dexamethasone-induced muscle atrophy via inhibiting NLRP3/GSDMD pathway-mediated pyroptosis. *Cell Death Discov*. 2021;7(1):251. doi:10.1038/s41420-021-00648-0
52. Zhang MY, Jiang YX, Yang YC, et al. Cigarette smoke extract induces pyroptosis in human bronchial epithelial cells through the ROS/NLRP3/caspase-1 pathway. *Life Sci*. 2021;269:119090. doi:10.1016/j.lfs.2021.119090
53. Liao K, Lv DY, Yu HL, Chen H, Luo SX. iNOS regulates activation of the NLRP3 inflammasome through the sGC/cGMP/PKG/TACE/TNF-α axis in response to cigarette smoke resulting in aortic endothelial pyroptosis and vascular dysfunction. *Int Immunopharmacol*. 2021;101(Pt B):108334. doi:10.1016/j.intimp.2021.108334
54. Xu W, Wang H, Sun Q, et al. TXNIP-NLRP3-GSDMD axis-mediated inflammation and pyroptosis of islet β-cells is involved in cigarette smoke-induced hyperglycemia, which is alleviated by andrographolide. *Environ Toxicol: Int J*. 2024;39(3):1415–1428. doi:10.1002/tox.24046